ASTRONOMY
AND
ASTROPHYSICS

*Letter to the Editor*

# WSRT observations of the Hubble Deep Field region

**M.A. Garrett[1], A.G. de Bruyn[2,4], M. Giroletti[1,3], W.A. Baan[2], and R.T. Schilizzi[1]**

[1] Joint Institute for VLBI in Europe (JIVE), Postbus 2, 7990 AA, Dwingeloo, The Netherlands (garrett@jive.nl)
[2] Netherlands Foundation for Research in Astronomy (ASTRON/NFRA), Postbus 2, 7990 AA, Dwingeloo, The Netherlands
[3] Dipartimento di Fisica dell Universita di Bologna, via Irnerio 46, 40126, Bologna, Italy
[4] Kapteyn Astronomical Institute, Postbus 800, 9700 AV Groningen, The Netherlands

**Abstract.** We present deep WSRT 1.4 GHz observations of the Hubble Deep Field region. At the $5\sigma$ level, the WSRT clearly detects 85 regions of radio emission in a $10' \times 10'$ field centred on the HDF. Eight of these regions fall within the HDF itself, four of these are sources that have not previously been detected at 1.4 GHz, although two of these are VLA detections at 8.5 GHz. The two new radio sources detected by the WSRT are identified with relatively bright ($I < 21^m$) moderate redshift spiral and irregular type galaxies. In the full field, the WSRT detects 22 regions of emission that were not previously detected by the VLA at 1.4 GHz. At least two of these are associated with nearby, extended star-forming galaxies.

**Key words:** galaxies: starburst – galaxies: active – radio continuum: galaxies

## 1. Introduction

Observations of the Hubble Deep Field (HDF) region (Williams et al. 1996, hereafter W96) at centimeter wavelengths are now advancing our understanding of the nature of the faint, microJy radio source population (Richards et al. 1998, hereafter R98; Richards et al. 1999, hereafter R99; Richards 2000, hereafter R00, and Muxlow et al. 1999, hereafter M99). These observations suggest that $\sim$ 60% of faint sub-mJy and microJy radio sources are identified with low radio luminosity ($L < 10^{23}$W/Hz), steep spectrum, moderate redshift ($z \sim 0.2$–1) star forming galaxies. These sources are often identified with morphologically peculiar, merging or interacting galaxies, with blue colours, and HII-like emission spectra (R98). The remaining 20% of the faint radio population are identified with relatively low-luminosity AGN and 20% are optically faint sources with no detections down to I=25.5 in the HFF and I=28.5 in the HDF. These optically faint systems are thought to be distant galaxies, obscured by dust (R99). The vast majority of far infrared ISO detections in the HDF (and the adjacent Hubble Flanking Fields, HFF) are also detected in

*Send offprint requests to*: M.A. Garrett

the radio (Aussel et al. 1999, hereafter A99), suggesting that the same strong correlation between the far infrared and radio continuum flux densities (as observed for nearby star-forming galaxies - see Condon 1992 and references therein) also holds for these fainter, more distant systems Barger et al. 2000.

In order to further advance the study of the faint microJy radio source population, we observed the HDF and the surrounding flanking fields (HFF) with the recently upgraded Westerbork Synthesis Radio Telescope (WSRT) at 1.4 GHz.

## 2. WSRT observations and data analysis

Observations of the HDF region were made with the upgraded WSRT at 1.38 GHz in the period from 20 April until 6 May 1999. A total of six (uninterrupted) 12 hour observations were made with different array configurations resulting in an excellent uv-coverage with baselines ranging from 36 to 2760 meters (with an increment of 12 meters). The WSRT continuum back-end provided 8 contiguous 10 MHz bands running from 1340–1420 MHz. The visibilities were averaged over 60 seconds. Full polarization information was obtained but is not presented here.

The data analysis was performed in NEWSTAR (Noordam, 1993) following the standard WSRT processing route. 3C286 was observed once per 12 hour run, and the complex gain solutions thus determined, were transferred to the HDF data. Typically, about 90% of the data proved to be of good and usable quality. The standard WSRT taper was applied to the data and baselines shorter than 100 meter were not used in the image, effectively filtering out large scale $> 5'$ emission features of both instrumental and galactic (foreground) origin. Images of $2048 \times 2048$ pixels covering an area of $2.8° \times 2.8°$ were generated. The brightest 121 sources in the field, with flux densities ranging from a high of 130 mJy down to 0.35 mJy, were used to self-calibrate the data (with a 60 second solution interval), and then subtracted from the uv-data. The central $900 \times 900$ pixels in the residual image was then cleaned down to a level of $28\,\mu$Jy yielding 8000 clean components. These were restored with a Gaussian beam with half-width $14.3'' \times 15.5''$ (RA $\times$ DEC). On top of this image we restored
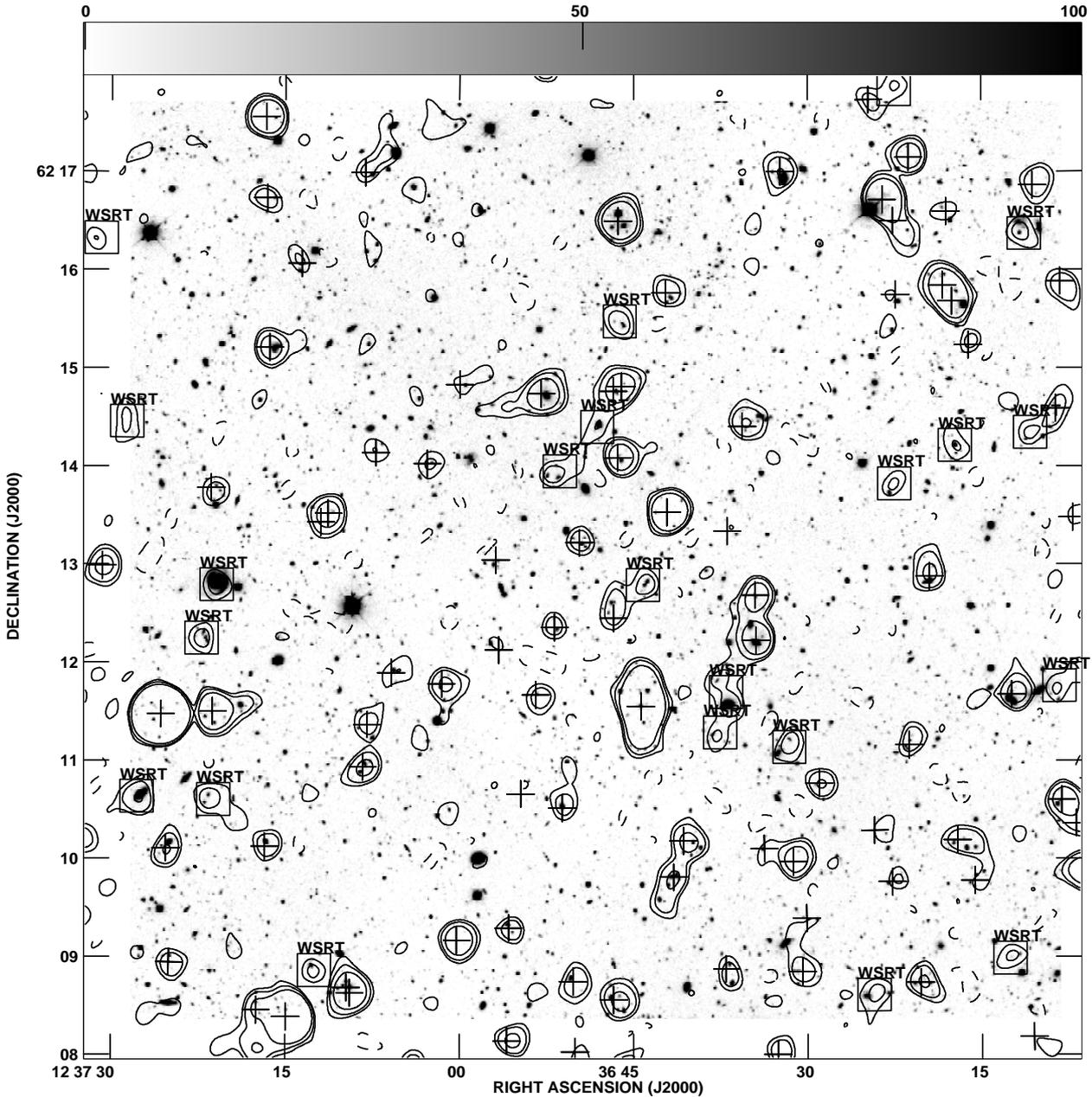
**Fig. 1.** The WSRT image of the HDF (inner $2.5'$) and HFF regions (a $10' \times 10'$ field), restored with a $15''$ circular beam and superimposed upon the deep CFHT I-band image of Barger et al. 1998. The $1\sigma$ rms noise level is $\sim 9$ microJy/beam with contours drawn at -3, 3, 5 and $10\sigma$. Crosses represent sources detected by the VLA at similar rms noise levels (R00). Sources detected by the WSRT (but not the VLA or MERLIN at 1.4 GHz) are boxed and appropriately labeled.

the self-calibration model, after first multiplying the residual image with a factor 1.2 to correct for self-calibration noise bias (Wieringa 1992). The full field has a r.m.s. noise level that varies from about 7.5 to $8\,\mu$Jy/beam, almost identical to the $7.5\,\mu$Jy noise level of the 1.4 GHz VLA image (R00). The local noise level around the strongest off-axis sources is affected by (we presume) pointing problems, however, all these sources are located outside the central $10' \times 10'$ region. Towards the centre of the image the noise appears to go up slightly. We attribute this to source confusion estimated at $5\,\mu$Jy/beam which, when

added in quadrature, raises the noise level to about $9\,\mu$Jy/beam in the central region of the field (this noise component is not significant beyond a radius of $0.3°$ due to the primary beam attenuation). Support for this interpretation comes from the extremely uniform noise level of $7.5\,\mu$Jy in the Stokes Q image.

The final total intensity image of the central HDF and HFF region is presented in Fig. 1, superimposed upon the deep CFHT I-band image of Barger et al. 1998. This $10' \times 10'$ WSRT image is corrected for primary-beam attenuation and is centred on the HDF. The HDF/HFF WSRT image was exported from NEW-

**Table 1.** WSRT 1.4 GHz HDF source list

| Source | RA (+12 hr) (h,m,s) | DEC (+62°) (° ′ ″) | $S_P$ $\mu$Jy | $S_T$ $\mu$Jy | Size (″ × ″, °) | $S_{VLA_{1.4}}$ $\mu$Jy | $S_{VLA_{8.5}}$ $\mu$Jy | $S_{15\mu}$ $\mu$Jy | $z$ |
|---|---|---|---|---|---|---|---|---|---|
| 3644+1247 | 36 44.190 | 12 47.31 | $67 \pm 7$ | $73 \pm 12$ | $< 13$ | - | 10 | 282 | 0.555 |
| 3644+1133 | 36 44.229 | 11 33.68 | $1190 \pm 14$ | $1606 \pm 14$ | $< 15$ | 1290 | 477 | - | 1.050 |
| 3646+1405 | 36 46.019 | 14 05.63 | $187 \pm 5$ | $187 \pm 5$ | $< 15$ | 179 | 168 | 107 | 0.962 |
| 3646+1236 | 36 46.284 | 12 36.03 | $64 \pm 6$ | $167 \pm 22$ | $32 \times 6, 140$ | - | - | - | 0.321 |
| 3647+1427 | 36 47.839 | 14 27.02 | $47 \pm 6$ | $116 \pm 21$ | $< 50$ | - | 9.8 | 307 | 0.139 |
| 3649+1314 | 36 49.575 | 13 14.12 | $68 \pm 4$ | $68 \pm 4$ | $< 15$ | 49 | 14 | 320 | 0.475 |
| 3651+1357 | 36 51.359 | 13 57.04 | $64 \pm 7$ | $82 \pm 14$ | $< 18$ | - | - | 151 | 0.557 |
| 3651+1222 | 36 51.811 | 12 22.37 | $57 \pm 5$ | $57 \pm 5$ | $< 15$ | 49 | 16 | 48 | 0.401 |

STAR to AIPS and source positions were fitted using the task IMFIT. Regions of emission with a measured peak flux density in excess of the assumed $5\sigma$ noise level ($45\,\mu$Jy) are considered to be bona fide detections. Note that the most negative feature in the analysed area has a flux density of $-42\,\mu$Jy. In principle, the accuracy with which we can determine the absolute position of the faintest unresolved radio sources in the field is $\sim 1.5''$ (1/10 of the restoring beam). For extended regions of emission this formal error is rather optimistic, and for the purposes of optical identifications, we adopt a positional error of $3''$.

## 3. Radio sources in the central HDF region

Within the central HDF region the WSRT detects eight radio sources. Their positions, flux densities and sizes are presented in Table 1. In most cases the deconvolved sizes (major axis, minor axis, PA) are upper-limits since the sources are smaller than the WSRT beam. The 1.4 and 8.5 GHz VLA flux densities (R98, R00), ISO ($15\,\mu$m) flux densities (A99), and the spectroscopic redshifts (Cohen et al. 2000, hereafter C00) of the sources are also presented.

Five of these detections (3644+1247, 3644+1133, 3646+1405, 3649+1314, and 3651+1222), are clearly associated with sources detected at the $5\sigma$ level by either the VLA at 8.5 GHz (R98) or the VLA/MERLIN at 1.4 GHz (see R00, M99 & Table 1). Their optical identifications are discussed in R98. In addition, 3647+1427 is clearly associated with the $4\sigma$ VLA 8.5 GHz source 3648+1427 (from the supplemental radio source catalogue of R98). Note that there is no formal VLA 1.4 GHz detection of 3644+1247, 3646+1236, 3647+1427, or 3651+1357. In the remainder of this paper we attempt to determine optical identifications for sources in the HDF region that are only detected by the WSRT. We employ the standard likelihood ratio (LR) analysis of Masci et al. 2000 (and references therein). We have compared the WSRT radio source positions in the HDF with the HDF HST Catalogue (W96), and in the HFF with the deep I-band catalogue of Barger et al. 1998 (hereafter B98). The spectroscopic redshifts referred to throughout this paper are taken from Cohen et al. 2000. We assume an error in the source positions of $3''$ in the radio and $0.5''$ in the optical.

One very extended region of emission, 3646+1236, is not detected by the VLA at 8.5 GHz but some fraction of the WSRT emission may be associated with VLA J123646+621226. However, the centroid of this extended region lies $10''$ to the north of the 1.4 GHz VLA source. The most likely optical identification of 3646+1236 (identification probability, $P > 72\%$) is with 4–241 (W96), a bright ($I \sim 20.6^m$), irregular (possibly merging), $z = 0.321$ galaxy lying within $\sim 3.5''$ of the radio centroid. Although there is no ISO detection in this area, the morphology of the optical identification suggests that the steep spectrum radio emission ($\alpha < -1$) is generated by star formation. If half the total radio emission in this area is associated with 3646+1236 itself, then following Haarsma et al. 1999 (and assuming a Salpeter IMF), we derive an upper-limit to the K-corrected star formation rate (SFR) of 17 M$_\odot$ yr$^{-1}$ (taking $q_0 = 0.5$, H$_0 = 50$ km/sec/Mpc).

3651+1357 is not detected by either the VLA at 8.5 GHz or the VLA/MERLIN at 1.4 GHz. The most likely optical identification ($34\% < P < 60\%$) is 2–652.0 (W96), a bright ($I \sim 20.6^m$), Sbc galaxy lying $4.4''$ to the south-east of the radio centroid with a spectroscopic redshift $z = 0.557$. There is an ISO $15\,\mu$m detection in this area (A99) also identified with 2–652.0 (Mann et al. 1997). The non-detection of 3651+1357 in the $10''$ resolution 8.5 GHz VLA image (R98), implies a steep radio spectral index ($\alpha \sim -1$). The coincident WSRT and ISO detections suggest that 2–652.0 is a star-forming galaxy. We derive an upper-limit to the K-corrected SFR of 38 M$_\odot$ yr$^{-1}$, in good agreement with the ISO estimate (Rowan-Robinson et al. (1997)).

There is one source in the HDF central region (VLA J123656+621302, a $z = 0.474$ elliptical galaxy, R98) that is detected by the VLA at 1.4 and 8.5 GHz ($S_{1.4} \sim 49.5\,\mu$Jy, $S_{8.5} = 8\,\mu$Jy) but not by the WSRT, even at the $3\sigma$ level (the WSRT peak flux in this region is $13\,\mu$Jy/beam). An inspection of each of the six 12 hour WSRT runs shows no emission in this region, suggesting that this source may be variable on a time-scale of months or years. R98 identify this source as a probable low-luminosity AGN. Very little is known about the radio variability properties of faint AGN, but assuming such sources are self-absorbed, for a given magnetic field strength, fainter sources should also be smaller sources. In the $10' \times 10'$ field considered here, only one other VLA 1.4 GHz detection (VLA J123654+621039, $S_{1.4} = 48\,\mu$Jy) is not detected by the WSRT below the $3\sigma$ level (the WSRT peak flux density in this region is $22\,\mu$Jy). We have been unable to identify a plausible optical

identification for this source from the VLA position. Given that radio variability in distant star-forming galaxies seems unlikely, this source is also a potential AGN candidate.

### 3.1. Detections in the HFF region

A complete radio catalogue of sources in the WSRT HDF and HFF region (including optical identifications) is in preparation (a preliminary catalogue is online at www.jive.nl/~mag/hdf). 85 distinct regions of emission are clearly detected with the WSRT above the $5\sigma$ limit within a $10' \times 10'$ field centred on the HDF. Of these 85 regions of emission, 55 are associated with discrete, single component VLA 1.4 GHz sources, 8 are associated with multiple VLA 1.4 GHz sources (for the WSRT these blend together to form a complex region of extended emission), and 22 are clearly detected by WSRT alone. As discussed earlier, some fraction of these WSRT-only detections are blends of sources that are presumably resolved by the higher resolution VLA/MERLIN 1.4 GHz observations. However, some fraction of the WSRT-only detections are clearly discrete sources and some of these are identified with bright, nearby galaxies.

An inspection of Fig 1 highlights two clear cases of this: 3720+1247 - coincident and clearly identified ($P > 99\%$) with an $I \sim 18.4^m$, z=0.106 spiral galaxy, and 3636+1132 - coincident and clearly identified ($P > 99\%$) with a $I \sim 18.6^m$, z=0.078 spiral galaxy. The latter source falls within the region surveyed by ISO and is coincident with a ISO $15\,\mu$m detection (A99). These two sources have radio powers that are a factor of $\sim 2$ higher than the typically brightest extragalactic radio supernovae (Wilkinson & de Bruyn, 1990) and in principle, they could be recent radio SNe that have sharply increased in flux density over the 2.5 years that separate the VLA and WSRT observations. However, we consider it more likely that these detections are cases of resolved extended disk emission. If all the radio emission associated with these sources is due to star formation, we estimate modest SFRs of 5 $M_\odot\,\mathrm{yr}^{-1}$ for 3720+1247 and 3 $M_\odot\,\mathrm{yr}^{-1}$ for 3636+1132. The fact that they are not detected by the VLA at 1.4 GHz, suggests that the radio emission could arise from a substantial area of the optical disk ($> 5$–$10$ kpc across).

## 4. Conclusions

Deep 1.4 GHz WSRT observations have detected 2 new radio sources in the HDF. These are associated with moderate redshift star-forming galaxies. In the full $10' \times 10'$ field, 22 new regions of radio emission are detected by the WSRT that are presumably resolved out by the VLA/MERLIN. At least two of these are clearly associated with relatively bright, nearby star-forming galaxies with modest SFRs. Further analysis of the full field is required to distinguish how many of the remaining regions are associated with discrete, extended radio sources, and how many are blends of closely separated, faint radio sources confused in the WSRT beam. The non-detection of 2 sources previously detected by the VLA at 1.4 GHz, hints at variability in the microJy AGN radio source population.

## References

Aussel, H., Cesarsky, C.J., Elbaz, D., Starck, J.L. 1999, A&A 342, 313.

Barger, A.J., Cowie, L.L., Trentham, N., Fulton, E., et al. 1998, AJ 117, 102.

Barger, A.J., Cowie, L.L., Richards, E.A. 2000, AJ 119, 2092.

Cohen J. G., Hogg D. W., Blandford R., et al. 2000, ApJ in press (astro-ph/9912048).

Condon, J.J. 1992, ARA&A 30, 575.

Haarsma, D. B., Partridge, R. B., Waddington, I., Windhorst, R. A. 2000, Procs. of the Texas Symposium on Rel. Astrophysics, in press (astro-ph/9904036).

Hogg D.W., Pahre M.A., Adelberger K.L., et al. 2000, ApJS 127, 1.

Mann, R.G., Oliver, S.J., Serjeant, S.B.G., Rowan-Robinson, M., et al. 1997, MNRAS 289, 471.

Muxlow, T.W.B. Wilkinson, P.N., Richards, A.M.S., et al. 1999, New Astronomy Reviews, 43, 623.

Masci, F.J., Condon, J.J, Barlow, T.A., et al. 2000, submitted to PASP (astro-ph/0002490)

Noordam, J.E., The NEWSTAR Cookbook, see www.nfra.nl/~wsrt.

Richards, E.A. 2000, ApJ 533, 611.

Richards, E.A., Kellermann, K.I., Fomalont, E.B., et al. 1998, AJ 116, 1039

Richards, E.A., Fomalont, E.B., Kellermann, K.I., et al. 1999, ApJ 526, L73.

Rowan-Robinson, M., Mann, R.G., Oliver, S.J., Efstathiou, A., et al. 1997, MNRAS 289, 490.

Wieringa, M.H. 1992, Experimental Astronomy 2, 203.

Wilkinson, P.N. & de Bruyn, A.G., 1990, MNRAS 242, 529.

Williams, R.E., Blacker, B, Dickinson, M. et al. 1996, AJ, 112, 1335.